https://doi.org/10.5194/egusphere-2026-797
Preprint. Discussion started: 6 March 2026

Implementation of the reduced complexity model InMAP at urban scale using a high-resolution WRF-Chem simulation

Diego Roberto Rojas Neisa[1], Alejandro Piracoca-Mayorga[1], Sebastian Espitia-Cano[1], and Ricardo Morales Betancourt[1]

[1]Department of Civil and Environmental Engineering, Universidad de los Andes, Cra. 1A 18 - 5, Bogota, Colombia

Correspondence: Ricardo Morales Betancourt (r.moralesb@uniandes.edu.co)

Abstract. Most of the population globally lives in areas exceeding prior and current WHO guidelines for fine particulate matter ($PM_{2.5}$), highlighting the persisting need for implementing emission reduction strategies. Given the complex transport and transformation processes that airborne species undergo in the atmosphere, chemical transport models can aid in designing and prioritizing air pollution mitigation actions. However, detailed chemical transport models often require substantial computational power and expertise. For that reason, reduced complexity models have emerged as an alternative, incorporating some of the information from chemical transport models while drastically reducing the technical complexity and computational demand. In this work, we build a local implementation of the Intervention Model For Air Pollution, InMAP, at high spatial resolution for a large urban area, in Bogotá, Colombia. As input for the reduced complexity model, we carried out a detailed 12-month simulation with the Weather Research and Forecasting model coupled with Chemistry (WRF-Chem) version 4.1. To achieve sufficiently high spatial-resolution for urban air quality, the model was configured with three nested domains of 27x27 km, 9x9 km, and 3x3 km respectively. When compared with surface station data, the modeled annual mean $PM_{2.5}$ showed a +3.3% overestimation at the city-scale. Furthermore, the WRF-Chem simulation accurately captured the structure of the observed $PM_{2.5}$ time series at daily, weekly and seasonal time-scales. The InMAP base fields showed a slight under-prediction relative to WRF-Chem, but overall, the correlation between the WRF-Chem and InMAP modeled $PM_{2.5}$ fields was high, with $R^2 = 0.92$. InMAP sensitivity was tested for three emission reduction scenarios of varying complexity, by comparing the marginal concentrations against simulations with the full chemical transport model. The scenarios ranged in complexity, from primary-PM reductions only, to scenarios exploring moderate and severe city-wide emissions reductions from diesel powered mobile sources. Although InMAP marginal $PM_{2.5}$ fields were linearly correlated with the corresponding WRF-Chem sensitivities, a strong overestimation in predicted $PM_{2.5}$ variations were shown for all emission reduction scenarios considered. For the simpler scenarios where only primary PM was reduced InMAP sensitivity was a factor of 2 that of WRF-Chem, while for the more complex emission reduction scenarios involving also reduction in gas-phase emissions, InMAP overestimated $PM_{2.5}$ concentrations by a factor of 5. The driver in InMAPs overestimated $PM_{2.5}$ sensitivity in the scenarios involving gas-phase precursors was a large overestimation of secondary organic aerosols and particulate nitrate. The results of this work suggest that InMAP can be used to scan for potential emission reduction scenarios at the urban-scale, specially when those scenarios involve mostly primary PM emission reductions. However, our analysis indicates that studies aiming to carry out assessments using the

https://doi.org/10.5194/egusphere-2026-797
Preprint. Discussion started: 6 March 2026

absolute reductions in concentration from InMAP should first calibrate its sensitivities against a full chemical transport model run.

1 Introduction

Exposure to air pollutants, especially to fine particulate matter ($PM_{2.5}$), negatively impacts human health, with estimates indicating several million excess deaths globally are attributable every year to poor air quality (e.g., Burnett et al., 2018). Both, chronic and episodic exposure to PM is associated with increased mortality (e.g., Chen and Hoek, 2020; Orellano et al., 2020). Multiple emission sectors contribute to the $PM_{2.5}$ concentration, with the relevance of different sources varying regionally (McDuffie et al., 2021). Despite the progress that has been achieved in some regions of the world in reducing particulate pollution, most of the population globally, specially in low- and middle-income countries, still experience fine particulate concentration at levels much higher than the WHO guidelines (Brauer et al., 2016). Therefore, continued efforts to reduce atmospheric emissions are necessary to reduce the negative health burden of air pollution.

Given the complex atmospheric chemistry and transport processes that determine the levels of air pollution at any given location, emission reductions in a specific site or sector might have varying degrees of impact over air pollutants concentrations elsewhere. Therefore, sensible emission reduction policies must consider not only primary emissions, but how atmospheric transport and transformation dictate its air pollution impact. The tool most suited to address the interactions resulting from atmospheric processes are comprehensive chemical transport models, or CTMs. These state-of-the-science models, which involve mechanistically resolving atmospheric transport, gas-phase chemistry, aerosol transformations, and other processes have undergone continuous development over more than 2 decades. Multiple comprehensive CTMs are currently available, including CAM-Chem (Emmons et al., 2020), CMAQ (Appel et al., 2017), and WRF-Chem (Grell et al., 2005). Involving CTMs in the design of air pollution reduction strategies, although complex, can lead to science-based policies, likely enhancing the effectiveness of such policy if implemented. However, the high requirement for computational resources intrinsic to running CTMs and the expertise needed to set-up and execute such models are not always available to air quality managers and decision makers. To offset these limitations, simpler models, often termed reduced-complexity models (RCM) or reduced-form models, have been developed (e.g., Tessum et al., 2017; Heo et al., 2016; Gentry et al., 2023).

Among the key characteristics of reduced-complexity models is the drastic reduction in computing time and simpler input data structure requirements. These characteristics make RCM suitable for quickly scanning multiple emission reduction scenarios and to analyze their potential impact on air pollution. In this work we focus on the implementation and evaluation of the Intervention Model For Air Pollution, InMAP, (Tessum et al., 2017) RCM, which is designed to estimate the spatially resolved concentration changes resulting from marginal changes in emissions relative to a baseline scenario. Because long-term exposure to particulate matter has shown to have the strongest association with health outcomes, the model is designed to estimate the annual average variations in concentration resulting from marginal emission changes.

As with most other RCM, InMAP requires several orders of magnitude less computational resources compared to those of a full CTM (e.g., Goodkind et al., 2019). Yet, the main input necessary to build a version of InMAP consist of 3-dimensional

https://doi.org/10.5194/egusphere-2026-797
Preprint. Discussion started: 6 March 2026

time-varying meteorological and air pollution fields produced from a CTM for the specific modeling domain. InMAP has been utilized to determine source receptor matrices in the continental United States, referred to as InMAP-US (Goodkind et al., 2019), by informing the model with a 12 km spatial resolution WRF-Chem simulation (Tessum et al., 2015). Among the many applications of RCMs, they are often employed for scenario analysis. In the US, several RCMs, including InMAP-US, have been used to analysis the impact of widespread adoption of electric vehicles (e.g., Choma et al., 2020; Gentry et al., 2023). InMAP has also been implemented over China (InMAP-China) using the WRF-CMAQ CTM at a 36 km spatial resolution (Wu et al., 2021). Furthermore, a global implementation of InMAP (Global-InMAP) is currently available (Thakrar et al., 2022). For that implementation, the CTM information was provided by the global model GEOS-Chem, with a resolution of 2°x2.5°. Although valuable to understand large-scale impacts of emission reductions, such coarse spatial resolution is of little use when addressing local emission sources or regions where concentration gradients are large, due to spatial heterogeneity in emissions, topography, or population density, like those often found in compact urban areas. Despite those limitations, Global InMAP has been used to explore the contribution of external sources in large urban centers globally (Tessum et al., 2022). The spatial resolution of global CTMs is likely not sufficient to resolve intra-city air pollution gradients, and it is also likely that the emissions used in global CTMs often lack local emission data for many cities worldwide.

Contrary to its original aim, there have been very few implementations of InMAP in the global south, which encompasses precisely those regions were availability of state-of-the-science CTMs is scarcer and where emissions data might be missing. In this work, we partially address this issue by building a local implementation of InMAP for a large urban area in the global south. In this work, we implemented the InMAP for the city of Bogotá in Colombia (InMAP-BOG) and explore the population-weighted $PM_{2.5}$ reductions resulting from hypothetical scenarios. We built InMAP locally by carrying out a detailed high-resolution (3x3 km) 12-month simulation with the WRF-Chem chemical transport model as input for the reduced complexity model. Besides evaluating the model-to-model base case simulation, we also carried out sensitivity tests with the full CTM and tested the same scenarios with InMAP-Bog. With this work we aim to explore the ability of InMAP to scan high-resolution emission abatement policies and to inform air quality management options. To our knowledge, this is one of the first implementations of InMAP outside of China and the United States.

2 Methods

The methodology in this study involved three steps. The first, was completing a 1-year simulation with a chemical transport model at the desired spatial resolution and then assessing its skill to represent local air pollution. The second was to use the outcome of that detailed CTM simulation to build InMAP and to test its sensitivity against that of the full CTM simulation. The third step was to utilize InMAP to quickly scan spatially-resolved emission reduction scenarios for policy use.

2.1 Implementation of InMAP

Typically, atmospheric models explicitly solve coupled mass conservation equations involving advection and turbulent transport as well as chemical transformations and removal from the atmosphere through deposition. In InMAP approach, gas-phase

https://doi.org/10.5194/egusphere-2026-797
Preprint. Discussion started: 6 March 2026

and particulate pollutant concentrations are computed through an approximate steady-state solution to the continuity equation for a given species

$$\frac{\partial c_i}{\partial t} = \nabla \cdot (K \nabla c_i) - \nabla \cdot (\bar{\mathbf{v}} c_i) + r_i + E_i - d_i \quad (1)$$

where, c_i is the concentration of species "i", whose tendency, $\partial c_i / \partial t$, is determined by advection by the mean wind vector ($\bar{\mathbf{v}}$) as well as by turbulent atmospheric transport, quantified here by the turbulent mixing parameter K. Additionally, any given species can be produced or consumed by multiple chemical reactions, which are represented by the net formation rate of species r_i, and can be removed by wet and dry deposition to the surface (d_i). In Eq. 1 E_i is the emission rate of the species i, which can be from anthropogenic and natural sources. In its simplified approach, InMAP produces only annual average pollutant concentration fields. The chemical species considered by InMAP are primary $PM_{2.5}$, volatile organic compounds (VOCs), secondary organic aerosol (SOA), sulfur dioxide (SO_x), particulate sulfate (pSO_4), oxides of nitrogen (NO_x), particulate nitrate (pNO_3), ammonia (NH_3), and particulate ammonium (pNH_4). InMAP must be compiled by providing it with hourly outputs from a one-year simulation with a full CTM, which are used by InMAP steady-state solution algorithm to extract atmospheric properties necessary to infer annual mean concentration fields. For a full description of InMAP the reader is referred elsewhere (e.g., Tessum et al., 2017), but we provide here the key variables linking it with the driving CTM simulation. In its original implementation, InMAP was driven by WRF-Chem v3.4 as the CTM providing the detailed fields (Tessum et al., 2017), with a domain covering North America at a resolution of 12 km. In this work we used a different version of the same CTM, WRF-Chem version 4.1, to provide the detailed simulation needed by InMAP, and therefore closely followed the original InMAP implementation as described in that work. From the three-dimensional WRF-Chem hourly output fields, which were organized in daily files, the necessary input variables were extracted and provided to InMAP. The complete list of WRF-Chem variables used by the InMAP preprocessor and how they are used is reported in Table D1, which is reproduced from the description of InMAP-US (see Table S1 in Tessum et al. (2017)). In contrast to other implementations of InMAP, we used higher spatial resolution (3km x 3km) and used a locally developed anthropogenic emission inventory. Our analysis is focused on a specially understudied region in terms of atmospheric chemical transport modeling. The details of the modeling domain and the WRF-Chem configuration are provided below.

2.1.1 Modeling domain

The relevant domain in this study is a 480 x 480 km region with a resolution of 3 km x 3 km centered in the city of Bogotá (Figure A1). With its population estimated at 8 million, the city is one of the most densely populated in Latin America (Wheeler, 2015), and is located 2600 meters above sea level in the equatorial Andean region of South America. The urban buildup is compact, spanning only 380 km^2, and therefore, the gradient between dense-urban and rural land-use is sharp. Additionally, the topography surrounding the city is complex, with nearby mountains reaching up to 4000 m (Figure 3). According to the local air quality monitoring network, annual mean $PM_{2.5}$ was 17.2 $\mu g\ m^{-3}$ in 2018, exceeding the World Health Organization (WHO) guidelines (WHO, 2006). Furthermore, largely due to regional biomass burning emission and large-scale

https://doi.org/10.5194/egusphere-2026-797
Preprint. Discussion started: 6 March 2026

meteorological conditions, the city experiences significant seasonal variation in $PM_{2.5}$ and other air pollutants, with two annual concentrations peaks, the first between January to March, and the other in September and October (Mendez-Espinosa et al., 2019). The 24-hour $PM_{2.5}$ routinely exceeds the daily local limit of 37 μg m^{-3}, and consequently, exceeds many times over the WHO air quality guidelines for 24 hour exposures. Most of those exceedances occur in the south-west of the city were industrial sources and heavy duty traffic are prevalent (East et al., 2021). Concentrations are much lower from June to September.

2.1.2 Base Simulation with WRF-Chem

We used the Weather Research and Forecasting model coupled with Chemistry (WRF-Chem) version 4.1, a meteorological and chemical transport model (e.g., Grell et al., 2005; Fast et al., 2006; Powers et al., 2017) as the driver for the RCM InMAP. The model configuration used in this study closely follows that of previous studies (Ballesteros-González et al., 2022), which have shown good skill in reproducing observed concentrations. The main configuration parameters are summarized in Table 1. The selected aerosol scheme, particularly relevant given the focus of this study on $PM_{2.5}$, was the Modal Aerosol Dynamics model for Europe (MADE) (Ackermann et al., 1998) with a Secondary Organic Aerosol (SOA) formation mechanism based on the Volatility Basis Set approach (MADE-VBS) (Ahmadov et al., 2012). The MADE-VBS scheme uses 3 log-normal aerosol modes to describe the particles size distribution, including a nucleation, accumulation and coarse modes. The model accounts for SOA formation using the VBS approach, which groups organics species according to its volatility and uses partitioning theory to estimate a gas-phase and a particle-phase amount of organic species (Donahue et al., 2009), and couples it with the gas-phase chemistry scheme. RACM, the gas-phase chemistry mechanism, includes 78 chemical species and 214 gas-phase reactions (Stockwell et al., 1990, 1997).

Table 1. WRF-Chem model parameterization.

Parameter	Scheme	Reference
Microphysics	Lin et al.	Lin et al. (1983)
Longwave Radiation	RRTM	Mlawer et al. (1997)
Shortwave Radiation	Dudhia	Dudhia (1989)
Land Surface	Noah	Ek et al. (2003)
Planetary Boundary Layer	YSU	Hong et al. (2006)
Cumulus	Grell-Freitas	Grell et al. (2014)
Gas-phase Chemistry	RACM	Stockwell et al. (1997)
Aerosol Mechanism	MADE	Ackermann et al. (1998)
SOA Scheme	VBS	Ahmadov et al. (2012)

To achieve the sufficiently high spatial resolution necessary for urban air quality assessment in a compact city layout like the one in Bogota, WRF-Chem was configured with three nested modeling domains (Figure A1). For this, the one-way nesting method was used, in which the larger domains provide the boundary and initial conditions for the inner domains. Initial and boundary conditions for the outermost domain were obtained from the global chemical transport model CAM-Chem (Emmons et al., 2020), 0.9° x 1.25° (roughly 100 km x 125 km horizontal resolution) and 56 vertical levels, and mapped to the WRF-

https://doi.org/10.5194/egusphere-2026-797
Preprint. Discussion started: 6 March 2026

Chem domain boundaries. The three nested WRF-Chem simulations were used to downscale CAM-Chem fields to increasingly higher horizontal resolutions corresponding to 27x27 km, 9x9 km, and 3x3 km respectively. Since the study area is the city of Bogotá, we will focus exclusively on the highest-resolution domain. Details of the full modeling domain are included in Appendix A. The model was configured with 41 eta-coordinate vertical levels, with 14 of those allocated to the lowest 1 km layer closest to the surface. This configuration has been used successfully in the past for shorter 1-month simulations exploring biomass burning impacts in the region (e.g., Ballesteros-González et al., 2020; Ballesteros-González et al., 2022). The initial and boundary conditions for the meteorological fields were extracted from the National Center for Environmental Prediction Final Operation Global Analysis (NCEP-FNL) provided, which has a spatial resolution of 1° and 6-hourly temporal resolution (NCEP, 2000).

2.1.3 Emissions

For the urban perimeter of Bogotá we used detailed emissions from a locally-developed emission inventory for the year 2018 (Pachón et al., 2018). The Bogotá local emission inventory has a 1 km x 1 km resolution and includes emissions from commercial, mobile, and industrial sources. To accurately capture day-to-day variations in activity, we applied specific activity profiles for workdays, Saturdays, and Sundays or holidays. This was done for mobile, industrial and commercial sources. Similarly, to account for week-to-week activity changes and to capture seasonal changes in activity, the weekly ridership data from the public transport system was used as a proxy (Figure B1). For PM, re-suspended particulate matter (RPM) sources are included, as those have been shown to be a significant source of primary PM in the city. For RPM emissions, we applied a monthly mitigation factor linked to precipitation, which modulates such emissions when the road surface is wet Pérez-Peña et al. (2017).

Emissions outside of the urban perimeter, where no data from the local emission inventory is available, were extracted from the Emissions Database for Global Atmospheric Research version 4.3.1 (EDGAR V4.3.1) at 0.1°x0.1° horizontal resolution (Crippa et al., 2016). Given its relevance in the domain, we included biomass burning emissions from the Fire Inventory from NCAR, FINN version 1 (Wiedinmyer et al., 2011) for the three domains. FINN has hourly temporal resolution and spatial resolution of 1 km × 1 km. To correctly simulate the transport of biomass burning plumes emissions, which are injected at height, we used the 1-dimensional plume-rise model embedded into WRF-Chem (Grell et al., 2011). Although the innermost domain is located far from the main biomass burning sources in the region, its overall contribution to $PM_{2.5}$ is significant. However, those emissions will not be affected by potential emission reduction strategies at the city-scale.

Biogenic emissions are calculated online using the Model of Emissions of Gases and Aerosols from Nature, MEGAN (Guenther et al., 2012), with emissions rates varying according to meteorological variables.

2.2 Scenario analysis with InMAP

To assess the skill of InMAP to predict changes in air pollution associated with diverse emission reduction scenarios, we set-up three hypothetical emission reduction scenarios in which emissions from one specific sector were decreased (Table 2). For those scenarios, we also conducted simulations with the full WRF-Chem model, so a direct comparison of the sensitivity

https://doi.org/10.5194/egusphere-2026-797
Preprint. Discussion started: 6 March 2026

of InMAP to emission reductions to those of the full CTM could be completed. The scenarios were built spanning diverse characteristics, considering emission sectors that are relevant for the city, but also considering the complexity in the type of emissions reduced in a given scenario. Similar scenarios had been previously analyzed but simulations had been carried out for just a couple of months (Bonilla et al., 2023). The scenarios range from primary PM only reductions (i.e., no gas phase emission reductions) to more complex settings involving the removal of emissions from diesel-powered mobile sources. The latter reduces all emission fluxes associated with the diesel power mobile sources, including gas-phase species, primary PM and gas-phase secondary aerosol precursors.

Table 2. Description of testing emission scenarios.

Scenario	Description
RPM-100	Resuspended dust emissions set to cero
Diesel-10	10% reduction in diesel-powered mobile emissions
Diesel-100	100% reduction in diesel-powered mobile emissions

3 Results

3.1 WRF-Chem simulation performance

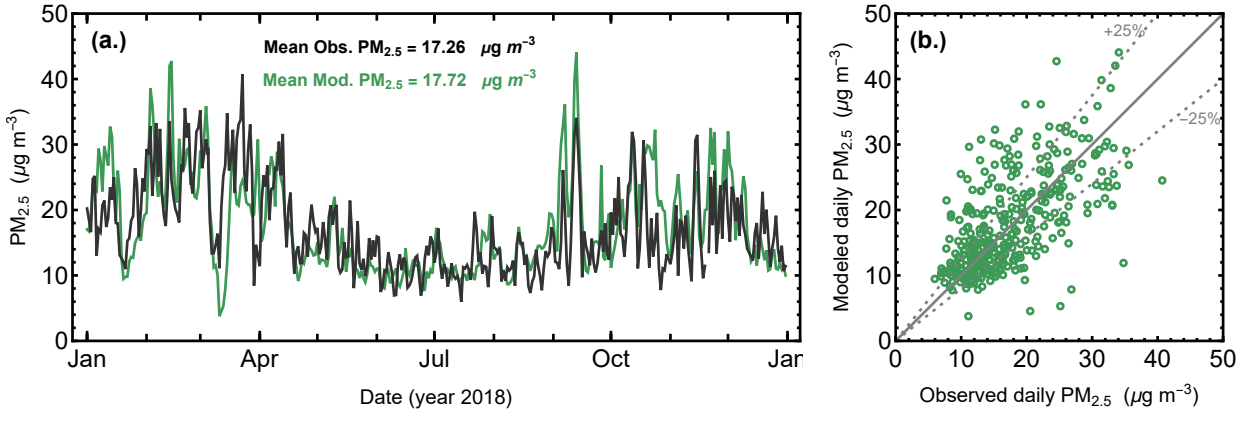

Figure 1. (a.) Time series of modeled (green) and observed (black) daily surface $PM_{2.5}$ concentration in the city of Bogota for 2018. (b.) Scatter plot of observed and modeled daily $PM_{2.5}$ concentration. The observed values are the means from the 13 active reference air quality monitoring sites displayed in the city.

The $PM_{2.5}$ concentration fields from the WRF-Chem simulation for the year 2018 showed close agreement with observations at different temporal scales. The modeled and observed timeseries of daily $PM_{2.5}$ for the city of Bogotá are shown in Figure 1a. The WRF-Chem simulation accurately captures the structure of the time series, including the annual cycle of concentration with

https://doi.org/10.5194/egusphere-2026-797
Preprint. Discussion started: 6 March 2026

higher concentrations mainly in January-March and peaking again in October-November. Week-to-week variations seem to be captured accurately by the model. Those variations are largely likely explained by regional events, but some local variations in emissions linked to city dynamics can contribute to the observed changes. The observed and modeled annual mean $PM_{2.5}$ for the city were 17.2 μgm^{-3} and 17.7 μgm^{-3}, respectively, demonstrating a slight +3.3% overestimation at the city-scale. Comparison of the standard deviation of daily concentration shows the model captured the variability of the $PM_{2.5}$ daily data. The standard deviation of modeled daily concentrations was 7.3 μgm^{-3}, in contrast to the observed standard deviation of 6.9 μgm^{-3}. At the daily scale, the R^2 for the model and observed data is 0.64 (Figure 1b). The time series from observations and from the model output.

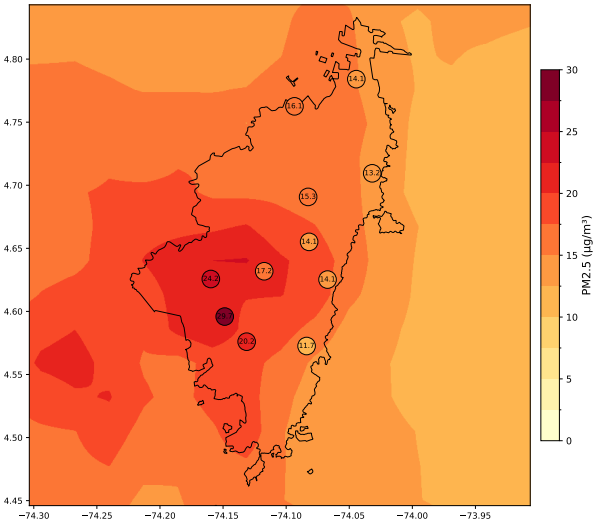

Figure 2. Annual mean spatial distribution of simulated $PM_{2.5}$ in a portion of the innermost domain containing the urban area of the city. The urban footprint is shown as the black contour. The observed annual mean $PM_{2.5}$ at the available air quality monitoring stations is also shown.

Although the urban area of Bogotá is relatively compact, intra-urban patterns in $PM_{2.5}$ distribution were also well represented in the simulations, with the model capturing the observed northeast-to-southwest concentration gradient (Figure 2). A statistical evaluation of the model performance in relation to established benchmarks (e.g., Emery et al., 2017) at individual air quality monitoring sites is shown in Appendix C. Overall, the results suggest the baseline WRF-Chem simulation is capable of reproducing the spatial and temporal variations in $PM_{2.5}$ at the urban scale in a way consistent with observations.

3.2 InMAP basline

The comparison of InMAP and WRF-Chem predicted $PM_{2.5}$ fields for the base simulation are shown in Figure 3. When analyzed over the entire D03 modeling domain, InMAP base $PM_{2.5}$ showed a relative error of just -4.6%, equivalent to a mean bias of -0.5 μg m^{-3}, implying InMAP slightly underestimates fine particulate matter. The bias is not spatially homogeneous,

https://doi.org/10.5194/egusphere-2026-797
Preprint. Discussion started: 6 March 2026

with the South-eastern portion of the domain, which is geographically located in the eastern plains of the country, showing an overestimation of $PM_{2.5}$ relative to WRF-Chem. Over the rest of the domain InMAP underestimates $PM_{2.5}$ fields relative to the full CTM simulation. Previous studies suggest that over the eastern lowlands, $PM_{2.5}$ is likely dominated by transport of biomass burning plumes from the eastern grasslands (Ballesteros-González et al., 2020). While most of the local sources are located west from the Andes.

Those two distinct regimes appear related to the topographic features of the domain, with the region of overestimation located on the low-lands east of the Andes mountain range.

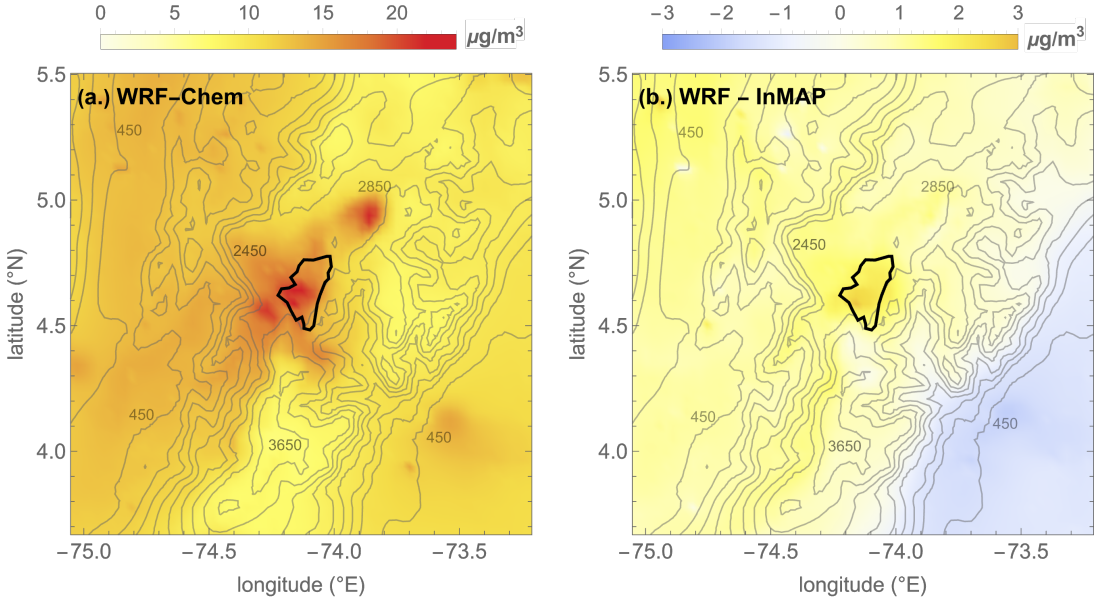

Figure 3. (a.) Annual mean $PM_{2.5}$ (in μg m^{-3}) for the inner most domain modeled with WRF-Chem, and (b.) Difference in annual mean $PM_{2.5}$ (in μg m^{-3}) between WRF-Chem and InMAP base case. Positive (negative) values in panel (b.) indicate underestimation (overestimation) by InMAP. The thick black contour depicts the urban area of Bogota. Terrain height contours in 400 m intervals are included in the graphic showing the complex topographic features of the domain.

When we restrict the analysis to the urban area of Bogota, InMAP base $PM_{2.5}$ had a -12.8% relative error, meaning it underestimated the variable by 2.0 μg m^{-3}. When analyzed in a scatter plot, the InMAP fields are strongly linearly correlated with those of WRF-Chem, with a correlation coefficient of 0.99 (for the urban area of Bogotá) and 0.91 for the entire D03 domain. Overall, the base case simulation by InMAP is accurate over the specified domain.

https://doi.org/10.5194/egusphere-2026-797
Preprint. Discussion started: 6 March 2026

3.3 InMAP sensitivity

The marginal fine particle concentration fields, $\Delta PM_{2.5}$, for each of the scenarios from Table 2 are shown in Figure 4. These marginal concentration fields can be regarded as the model sensitivity to the emission reductions that define each scenario. InMAP sensitivities were significantly larger than those of WRF-Chem, and the magnitude of the sensitivity of aerosol components to emissions was strongly dependent on the type of emission reduction scenario. For the RPM-100 scenario, which exclusively involves reductions in primary PM emissions, InMAP sensitivity $\Delta PM_{2.5}$ was on average two times larger than that of the full CTM.

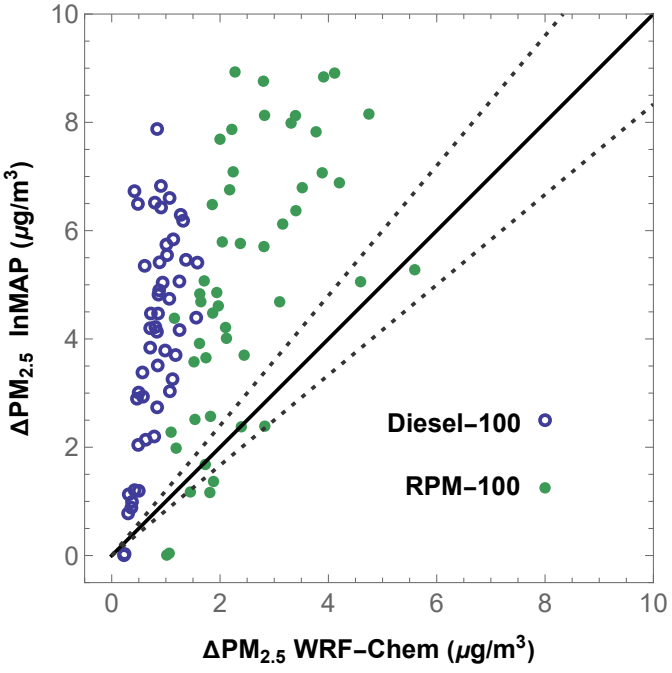

Figure 4. Scatter plot of the marginal $PM_{2.5}$ concentrations calculated with the full chemical transport model WRF-Chem ($\Delta PM_{2.5}$ WRF-Chem) and with the InMAP model ($\Delta PM_{2.5}$ WRF-Chem). The data shown is for the test scenarios in which resuspended dust emissions were removed (RPM-100) and for the one in which all diesel emissions from mobile sources were removed (Diesel-100).

The sensitivities for non-primary PM components vary significantly between InMAP and the full CTM. Particularly critical in our analysis was the large overestimation in the sensitivity of particulate nitrate and secondary organic aerosol (SOA) to precursor emissions. This was most notorious in the *Diesel-100* scenario, where the total $PM_{2.5}$ sensitivity was on average, 5.0 times that of WRF-Chem, implying a more severe overestimation compared with the simpler RPM scenario. The additional sensitivity was driven mostly by an excessive secondary aerosol yield in InMAP. Noticeably, in all the scenarios analyzed, the overestimation of the primary PM sensitivity was close to a factor of 2 relative to the WRF-Chem sensitivity. The consistency in this number indicates that InMAP's atmospheric transport efficiency is limited, causing that most of the emitted particle

https://doi.org/10.5194/egusphere-2026-797
Preprint. Discussion started: 6 March 2026

mass remains near the surface layer. Therefore, for the most complex emission reduction scenarios, the overestimation in marginal $PM_{2.5}$ seems to be driven by the reduced transport (roughly a factor of 2), and another overestimation factor from the overproduction of secondary aerosol species, mainly particulate nitrate and SOA.

The resulting marginal concentration fields from InMAP are moderately linearly correlated with those from WRF-Chem, with correlation coefficients of 0.60 for the RMP-100 test scenario and 0.59 for the Diesel-100 scenario. Therefore, despite the overestimation in the marginal concentration from emission reductions, the spatial patterns produced by InMAP are consistent with those of the full CTM. This indicates that InMAP can be used to assess the spatial footprint of specific emission reduction scenarios, and that with a proper calibration, can also be used to estimate absolute reductions, and then be used for health impact assessments.

In the moderate *10%-diesel* reduction scenario, the relative overestimation of SOA mass was much lower than in the *no-diesel* scenario. This suggests that scenarios with strong reduction in gas-phase precursors could be challenging for the InMAP model.

4 Conclusions

We implemented the reduced complexity model InMAP at a spatial resolution of 3km x 3km using a detailed atmospheric chemical transport simulation with the WRF-Chem model. The WRF-Chemm base simulation was shown to meet high quality criteria when compared to observed $PM_{2.5}$ concentrations at the city-scale, capturing variability at daily and seasonal scales, as well as the observed spatial patterns. In the base line simulation, we explored the application of weekly activity patterns, which improved the ability of the model to capture the observed variability of $PM_{2.5}$ fields at the city scale.

In addition to evaluating InMAP's baseline run, we also tested InMAP sensitivity by comparing it with a set of three emission reduction scenarios that were also simulated with the WRF-Chem chemical transport model. Overall, we found that InMAP overestimated marginal $PM_{2.5}$ for all emission reduction scenarios considered. For settings in which only primary PM was reduced, with no gas-phase species changes, InMAP predicted twice as large concentration reductions compared to WRF-Chem. However, the correlation between both models marginal concentration changes was high, suggesting the issue could be corrected with proper calibration.

For more complex emission reduction scenarios involving also reduction in gas-phase emissions, InMAP overestimated $PM_{2.5}$ concentrations more severely. The driver in InMAPs overestimated $PM_{2.5}$ sensitivity in the scenarios involving gas-phase precursors was a large overestimation of secondary organic aerosols and particulate nitrate.

Despite some of the limitations detected in this study, the computational efficiency of the reduced complexity model and the linear relation of its sensitivities to those of the full CTM, suggests this tool could useful for policy makers to quickly scan through potential emission reductions scenarios sorting them based on its efficacy in reducing exposure. This could allow to explore a large space of potential scenarios, quickly narrowing it to those with the largest potential benefits.

https://doi.org/10.5194/egusphere-2026-797
Preprint. Discussion started: 6 March 2026

Data availability. The model output, consisting of daily means of the WRF-Chem version 4.1, and the model configuration used to produce the results in this paper is archived on repository under DOI https://doi.org/10.71590/9RESNN (Morales Betancourt et al., 2026), which is available from the Datahub institutional repository of Universidad de los Andes (Bogotá, Colombia).

Appendix A: Model configuration and description of nested domains

The WRF-Chem model configuration was selected based on the skill shown on previous modeling studies over the same region (e.g., Ballesteros-González et al., 2020). The set of parameterization and physics option were already provided in Section 2.1.2.

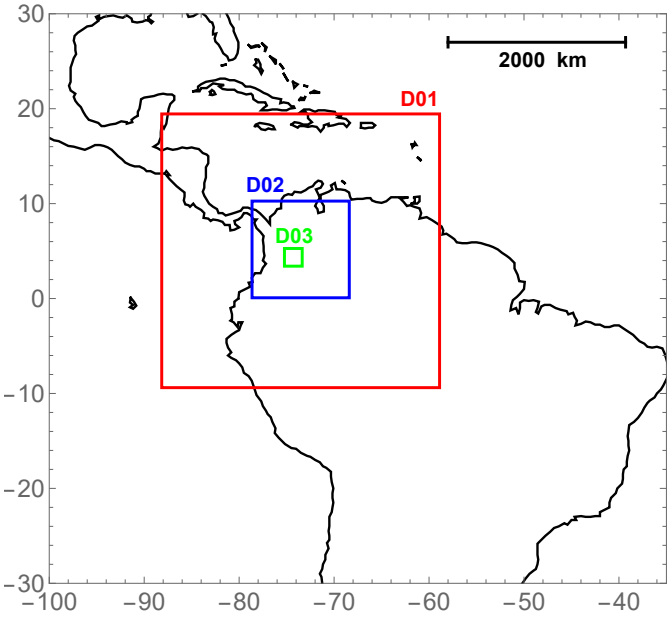

Figure A1. Geographic location of the three modeling domains used in this study in a latitude-longitude representation. Each nested domain has increasingly higher spatial resolution. Although the simulation was carried out for the 3 domains, only the results from the innermost (D03) are reported in this study.

To achieve sufficiently high spatial resolution for meaningful urban-scale modeling for the city of Bogota we configured the WRF-Chem model with three nested domains of increasing spatial resolution (Figure A1). The domains centered in the city of Bogota (lat. 5.194 – long. -73.522) have a horizontal resolution of 27x27 km (120x120 grid cells), 9x9 km (126x126 grid cells), and 3x3 km (69x69 grid cells) for domain 1 (D01), domain 2 (D02), and domain 3 (D03), respectively. Due to its relevance for urban-scale analysis, only the fields resulting from the the highest resolution domain, D03, were used in this work. Simulations were conducted for the entire year of 2018 for the three domains. The outermost domain (D01) is driven laterally by the meteorological and chemical-species fields from global chemical transport models, as described in the main text. The simulations for D01 were split in 3-month batches, corresponding to January-March, April-June, July-September, and October-December. Given the large domain size (roughly 3240 km x 3240 km) each 3-month batch was initialized with the

https://doi.org/10.5194/egusphere-2026-797
Preprint. Discussion started: 6 March 2026

global model fields three days prior to the initial analysis date, allowing for 72-hour of spin-up time. Numerical experiments for the three domains shared the same physical parameterizations.

https://doi.org/10.5194/egusphere-2026-797
Preprint. Discussion started: 6 March 2026

Appendix B: Local emissions and source activity patterns

Weekly activity variations

To account for significant variations in mobile source activity patterns throughout the year, we used the public transport system weekly ridership data reports as a proxy of mobile source activity. These reports are made publicly available by the the city's public transport authority. The activity factor we introduced in our emissions was defined such that it represents deviations from the average ridership, which was set to 1 (Figure B1).

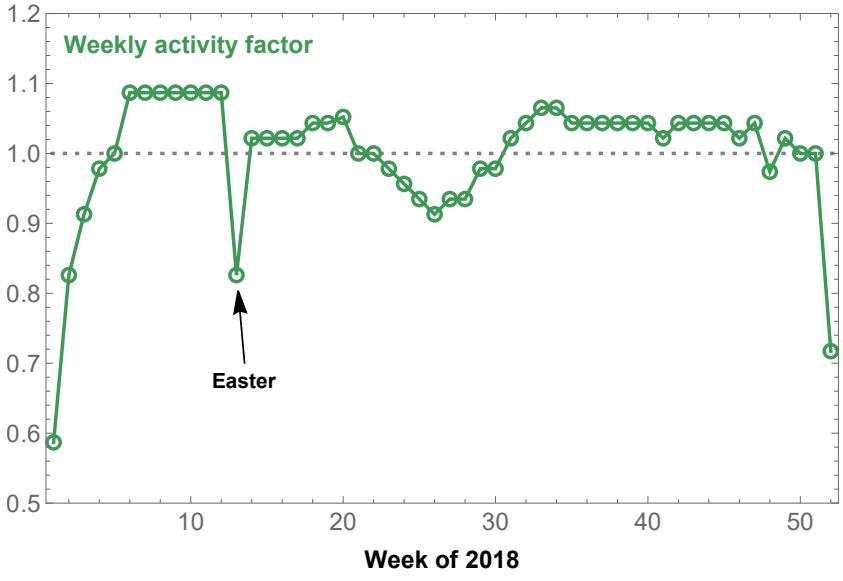

Figure B1. Normalized weekly activity factor, f_w, for mobile sources as inferred from ridership data from the city's public transport system. The factor was defined such that annual-mean activity is set to 1. When $f_w > 1$ it implies above-average activity, while $f_w < 1$ indicates below-average activity levels.

The sharp activity variations are well explained by some societal factors. The education sector (from elementary schools to universities) typically have holiday breaks in December-January and June-July. Additionally, many companies and government agencies have holidays from mid-December to mid-January. The ridership data captures the above described patterns, exhibiting large departures from the annual mean values for specific periods. On average, daily ridership in the public transport system for 2018 was 2.3 million trips. Minimum ridership is observed in the first week of the year (with 1.35 million trips per day) with a similar decline in the last week of the year. There is a decrease in activity during the religious holiday Easter, as Thursday and Friday of that week are national public holidays. We consider this approach as a good proxy of activity, and the method potentially useful for researchers elsewhere aiming to capture day-to-day and week-to-week variations in air quality simulations. Additionally, because of the strong daily activity variations within city, we also applied specific activity factors for weekdays, Saturdays, and Sundays (including public holidays).

https://doi.org/10.5194/egusphere-2026-797
Preprint. Discussion started: 6 March 2026

Local and global emission merging

The spatial scale of global emissions inventories is not suitable for urban-scale modeling applications. To circumvent that issue we used emissions from the local atmospheric emission inventory for the city limits of Bogota for year 2018, at 1x1km resolution, and merged it with the global emission inventory for those areas in D03 outside the city. If $B_{i,j}$ is the fraction of a given 3x3 km grid cell that has local emission data (i.e., the fraction of that grid cell that overlaps with the gridded local emission inventory of Bogota), then we merged the global and local emissions using

$$E_{i,j} = B_{i,j} \times E_{i,j}^{local} + (1 - B_{i,j}) \times E_{i,j}^{global} \quad \text{(B1)}$$

where $E_{i,j}^{local}$ is the flux of emissions from the local emission inventory for grid cell i, j, and $E_{i,j}^{global}$ is the flux for that cell from EDGAR. In this way, for model grid cells entirely inside the domain of the local emission inventory we use local emissions. For those cells completely outside the domain of the local emission inventory, then we use the global emissions. For the handful of *boundary* cells that partially overlap with the local emission inventory, then the emissions of both are combined according to Equation (B1).

https://doi.org/10.5194/egusphere-2026-797
Preprint. Discussion started: 6 March 2026

Appendix C: Statistical evaluation of the model skill

We applied multiple metrics to assess the model skill to represent fine particulate ($PM_{2.5}$) spatial and temporal distributions for the city of Bogota. Modeled daily mean $PM_{2.5}$ for the entire year 2018 were compared to available observations over the same period. There were 11 air quality monitoring sites with valid data (i.e., $> 75\%$ of valid data) to carry out the comparison for the simulation period. The metrics include:

$$NMB = 100 \times \frac{\sum (M_j - O_j)}{\sum O_j} \quad \text{(C1)}$$

$$NME = 100 \times \frac{\sum |M_j - O_j|}{\sum O_j} \quad \text{(C2)}$$

where M_j are model outputs and O_j are observations for a specif location j, and the summation is carried out over time, in this case, over model and observed daily-mean $PM_{2.5}$ concentrations. The results are shown in *soccer-goal* plots (NMB and NME metrics) and Taylor diagrams (modeled and observed standard deviation, and correlation coefficient, ρ). In this way, we assessed temporal correlation metrics, variability metrics, and bias-related metrics (Figure C1).

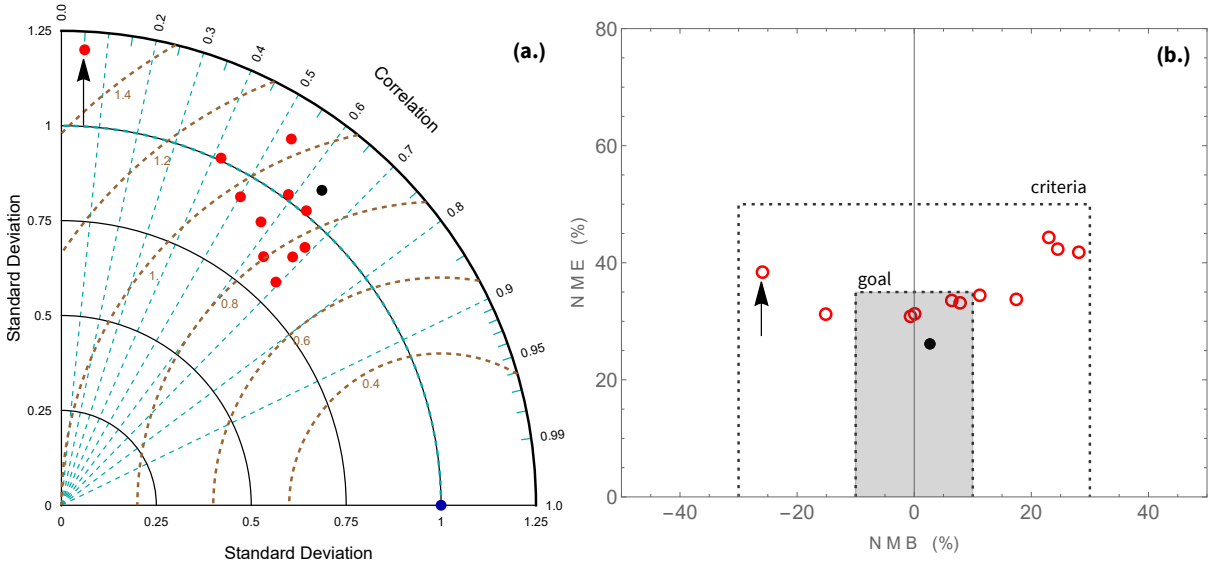

Figure C1. (a.) Taylor diagram for modeled and observed daily $PM_{2.5}$ data for the 11 stations with valid data (red points). The black circle represents the city-mean $PM_{2.5}$ timeseries. In this diagram, the *x* axis is the standard deviation (SD) normalized by the SD of the observed data. The dashed circles are the centered RMSE, also normalized by the observed SD. (b.) *Soccer-goal* plot showing the Normalized Mean Bias (NMB) and Normalized Mean Error (NME) for the same data set. The *goal* benchmark region is shaded in gray. The arrow is pointing to station S1, which was the only site with a correlation coefficient lower than the 0.4 criteria.

https://doi.org/10.5194/egusphere-2026-797
Preprint. Discussion started: 6 March 2026

C1 City-wide analysis

For this analysis we pooled together the daily-mean $PM_{2.5}$ concentrations from all the available monitoring sites to create a city-mean $PM_{2.5}$ time series. To create a comparable dataset from the model output, we averaged all the daily-means from the specific grid cells within the urban footprint of the city. At the city-mean scale, the model meets the performance goals for NMB and NME as specified in Emery et al. (2017), with NMB of +2% and NME of 27%. The correlation coefficient was 0.63, which is higher than the criteria of 0.4, but falls short of the *goal* performance threshold of 0.7. Results for the city-wide analysis are shown as the black circles in Figure C1. Our analysis was carried out for the 365 paired model and observed daily means.

C2 Intra-city variations

We evaluated the same model performance metrics for each individual monitoring site to determine the model's ability to capture intra-city variations in air quality fields. Figure C1b shows the NMB and NME for the model when evaluated against observations. The model met the bias and error criteria for the 11 stations analyzed Emery et al. (2017). Furthermore, The stricter *goals* where met for 4 out of 11 stations. Furthermore, as seen in Figure C1a, the model performance for 10 out of 11 monitoring sites met the correlation coefficient criteria $\rho > 0.4$, with the lone exception of an industrial monitoring site, which shows a distinctly different temporal structure to the other monitoring sites. The assessment of model performance reported here suggests the model configuration is capable of capturing intra-city gradients and temporal variations in this urban setting. The locations and annual mean $PM_{2.5}$ concentrations for the city's air quality monitoring sites is shown in Table C1.

Table C1. Air quality monitoring site information for those with valid $PM_{2.5}$ data for 2018. Stations are sorted in order of decreasing annual mean $PM_{2.5}$ concentration for the period. We include the Station ID, Annual mean $PM_{2.5}$ concentration, station location in lat. lon. coordinates, and the type of station.

Station ID	Annual mean $PM_{2.5}$ (μg m^{-3})	Lon. Degrees	Lat. Degrees	Type
Carvajal-Sevillana (S1)	29.7	-74.1487	4.59591	Industrial
Kennedy	24.2	-74.1597	4.62567	Background
Tunal	20.2	-74.1313	4.57599	Background
Puente Aranda	17.2	-74.1174	4.63182	Industrial
Suba	16.1	-74.0934	4.76255	Background
Las Ferias	15.3	-74.0826	4.69076	Traffic
Min. Ambiente	14.1	-74.0672	4.62523	Traffic
Guaymaral	14.1	-74.0444	4.7841	Background
CAR	14.1	-74.0818	4.65511	Background
Usaquen	13.2	-74.0318	4.70946	Background
San Cristobal	11.7	-74.0838	4.57256	Background

https://doi.org/10.5194/egusphere-2026-797
Preprint. Discussion started: 6 March 2026

Appendix D: WRF-Chem variables used in InMAP

Table D1. WRF-Chem variable names and their use in InMAP. The list presented here is identical to the one reported in Table S1 of the study describing InMAP first implementation (Tessum et al., 2017)

WRF-Chem variable	Description	Use in InMAP
hc5, hc8, olt, oli, tol, xyl, csl, cvasoa1, cvasoa2, cvasoa3, cvasoa4	Anthropogenic VOCs, SOA precursors	VOA/SOA partition
asoa1i, asoa1j, asoa2i, asoa2j, asoa3i, asoa3j, asoa4i, asoa4j	Antrhopogenig SOA	VOA/SOA partition
iso, api, sesq, lim, cvbsoa1, cvbsoa2, cvbsoa3, cvbsoa4	biogenic VOCs, SOA precursors	
bsoa1i, bsoa1j, bsoa2i, bsoa2j, bsoa3i, bsoa3j, bsoa4i, bsoa4j	biogenic SOA	
no, no2	NOx	NOx/pNO3 partition
no3ai, no3aj	Particulate Nitrate	NOx/pNO3 partition
so2, sulf	SO2 and sulfate	SOx/pSO4 partition
so4ai, so4aj	particulate SO4	SOx/pSO4 partition
nh3	Ammonia	NH3/pNH4 partition
nh4ai, nh4aj	Particulate Ammonia	NH3/pNH4
PM2_5_DRY	$PM_{2.5}$	Model evaluation
U, V, W	wind components	Advection and Mixing
PBLH	Planetary Boundary Layer Height	Turbulent Mixing
PHB and PH	Base geopotential and its perturbation	Layer heights
HFX	Surface Heath Flux	Dry deposition and Mixing
UST	Friction velocity	Dry deposition
T	Temperature	Reaction rates
PB, P	Pressure and perturbation pressure	Reaction rates
ho, h2o2	Radicals	Reaction rates
LU_INDEX	Land Use Index	Turbulent mixing
QRAIN	Rain water mixing ratio	Wet deposition
CLDFRA	Cloud fraction	Dry deposition
QCLOUD	Cloud water mixing ratio	Reaction rates
ALT	Inverse air density	Conversion factor
SWDOWN, GLW	Downward radiation at surface	Dry deposition

Author contributions. Diego Rojas: Conceptualization, Investigation, Software, Visualization, Writing - review and editing. Piracoca, A.: Conceptualization, Investigation, Writing - review and editing, Formal analysis. Espitia-Cano, S.: Investigation, Writing - review and editing. Morales Betancourt, R.: Conceptualization, Methodology, Writing - Original Draft, Investigation, Visualization, Funding acquisition. Simulations were designed by all co-authors and were carried out and analyzed by D. Rojas, and A. Piracoca.

Competing interests. The authors declare that they have no known competing financial interests or personal relationships that could have appeared to influence the work reported in this paper.

https://doi.org/10.5194/egusphere-2026-797
Preprint. Discussion started: 6 March 2026

Acknowledgements. This study was partially funded by the Center for Environmental Research (CIIA) from Universidad de los Andes.

https://doi.org/10.5194/egusphere-2026-797
Preprint. Discussion started: 6 March 2026

References

Ackermann, I. J., Hass, H., Memmesheimer, M., Ebel, A., Binkowski, F. S., and Shankar, U.: Modal aerosol dynamics model for Europe: development and first applications, Atmospheric Environment, 32, 2981–2999, https://doi.org/10.1016/S1352-2310(98)00006-5, 1998.

Ahmadov, R., McKeen, S. A., Robinson, A. L., Bahreini, R., Middlebrook, A. M., de Gouw, J. A., Meagher, J., Hsie, E.-Y., Edgerton, E., Shaw, S., and Trainer, M.: A volatility basis set model for summertime secondary organic aerosols over the eastern United States in 2006, Journal of Geophysical Research: Atmospheres, 117, https://doi.org/10.1029/2011JD016831, 2012.

Appel, K. W., Napelenok, S. L., Foley, K. M., Pye, H. O. T., Hogrefe, C., Luecken, D. J., Bash, J. O., Roselle, S. J., Pleim, J. E., Foroutan, H., Hutzell, W. T., Pouliot, G. A., Sarwar, G., Fahey, K. M., Gantt, B., Gilliam, R. C., Heath, N. K., Kang, D., Mathur, R., Schwede, D. B., Spero, T. L., Wong, D. C., and Young, J. O.: Description and evaluation of the Community Multiscale Air Quality (CMAQ) modeling system version 5.1, Geoscientific Model Development, 10, 1703–1732, https://doi.org/10.5194/gmd-10-1703-2017, 2017.

Ballesteros-González, K., Espitia-Cano, S. O., Rincón-Caro, M. A., Rincón-Riveros, J. M., Perez-Peña, M. P., Sullivan, A., and Morales Betancourt, R.: Understanding organic aerosols in Bogotá', Colombia: In-situ observations and regional-scale modeling, Atmospheric Environment, 284, 119 161, https://doi.org/https://doi.org/10.1016/j.atmosenv.2022.119161, 2022.

Ballesteros-González, K., Sullivan, A. P., and Morales-Betancourt, R.: Estimating the air quality and health impacts of biomass burning in northern South America using a chemical transport model, Science of The Total Environment, 739, 139 755, https://doi.org/https://doi.org/10.1016/j.scitotenv.2020.139755, 2020.

Bonilla, J. A., Aravena, C., and Morales-Betancourt, R.: Assessing Multiple Inequalities and Air Pollution Abatement Policies, Environmental and Resource Economics, 84, 695–727, https://doi.org/10.1007/s10640-022-00745-3, 2023.

Brauer, M., Freedman, G., Frostad, J., van Donkelaar, A., Martin, R. V., Dentener, F., Dingenen, R. v., Estep, K., Amini, H., Apte, J. S., Balakrishnan, K., Barregard, L., Broday, D., Feigin, V., Ghosh, S., Hopke, P. K., Knibbs, L. D., Kokubo, Y., Liu, Y., Ma, S., Morawska, L., Sangrador, J. L. T., Shaddick, G., Anderson, H. R., Vos, T., Forouzanfar, M. H., Burnett, R. T., and Cohen, A.: Ambient Air Pollution Exposure Estimation for the Global Burden of Disease 2013, Environmental Science & Technology, 50, 79–88, https://doi.org/10.1021/acs.est.5b03709, 2016.

Burnett, R., Chen, H., Szyszkowicz, M., Fann, N., Hubbell, B., Pope, C. A., Apte, J. S., Brauer, M., Cohen, A., Weichenthal, S., Coggins, J., Di, Q., Brunekreef, B., Frostad, J., Lim, S. S., Kan, H., Walker, K. D., Thurston, G. D., Hayes, R. B., Lim, C. C., Turner, M. C., Jerrett, M., Krewski, D., Gapstur, S. M., Diver, W. R., Ostro, B., Goldberg, D., Crouse, D. L., Martin, R. V., Peters, P., Pinault, L., Tjepkema, M., van Donkelaar, A., Villeneuve, P. J., Miller, A. B., Yin, P., Zhou, M., Wang, L., Janssen, N. A. H., Marra, M., Atkinson, R. W., Tsang, H., Thach, T. Q., Cannon, J. B., Allen, R. T., Hart, J. E., Laden, F., Cesaroni, G., Forastiere, F., Weinmayr, G., Jaensch, A., Nagel, G., Concin, H., and Spadaro, J. V.: Global estimates of mortality associated with long-term exposure to outdoor fine particulate matter, Proceedings of the National Academy of Sciences, 115, 9592–9597, https://doi.org/10.1073/pnas.1803222115, 2018.

Chen, J. and Hoek, G.: Long-term exposure to PM and all-cause and cause-specific mortality: A systematic review and meta-analysis, Environment International, 143, 105 974, https://doi.org/https://doi.org/10.1016/j.envint.2020.105974, 2020.

Choma, E. F., Evans, J. S., Hammitt, J. K., Gómez-Ibáñez, J. A., and Spengler, J. D.: Assessing the health impacts of electric vehicles through air pollution in the United States, Environment International, 144, 106 015, https://doi.org/https://doi.org/10.1016/j.envint.2020.106015, 2020.

https://doi.org/10.5194/egusphere-2026-797
Preprint. Discussion started: 6 March 2026

Crippa, M., Janssens-Maenhout, G., Dentener, F., Guizzardi, D., Sindelarova, K., Muntean, M., Dingenen, R. V., and Granie, C.: Forty years of improvements in European air quality: regional policy-industry interactions with global impacts, Atmospheric Chemistry ans Physics, 6, 3825–3841, https://doi.org/10.5194/acp-16-3825-2016, 2016.

Donahue, N. M., Robinson, A. L., and Pandis, S. N.: Atmospheric organic particulate matter: From smoke to secondary organic aerosol, Atmospheric Environment, 43, 94–106, https://doi.org/https://doi.org/10.1016/j.atmosenv.2008.09.055, atmospheric Environment - Fifty Years of Endeavour, 2009.

Dudhia, J.: Numerical study of convection observed during the winter monsoon experiment using a mesoscale two-dimensional model, Journal of the Atmospheric Sciences, 46, 3077–3107, https://doi.org/10.1175/1520-0469(1989)046<3077:NSOCOD>2.0.CO;2, 1989.

East, J., Montealegre, J. S., Pachon, J. E., and Garcia-Menendez, F.: Air quality modeling to inform pollution mitigation strategies in a Latin American megacity, Science of The Total Environment, 776, 145 894, https://doi.org/https://doi.org/10.1016/j.scitotenv.2021.145894, 2021.

Ek, M., Mitchell, K., Lin, Y., Rogers, E., Grunmann, P., Koren, V., Gayno, G., and Tarpley, J.: Implementation of Noah land surface model advances in the National Centers for Environmental Prediction operational mesoscale Eta model, Journal of Geophysical Research: Atmospheres, 108, https://doi.org/10.1029/2002JD003296, 2003.

Emery, C., Liu, Z., Russell, A. G., Odman, M. T., Yarwood, G., and Kumar, N.: Recommendations on statistics and benchmarks to assess photochemical model performance., Journal of the Air Waste Management Association, 67, 582–598, https://doi.org/10.1080/10962247.2016.1265027, 2017.

Emmons, L. K., Schwantes, R. H., Orlando, J. J., Tyndall, G., Kinnison, D., Lamarque, J.-F., Marsh, D., Mills, M. J., Tilmes, S., Bardeen, C., Buchholz, R. R., Conley, A., Gettelman, A., Garcia, R., Simpson, I., Blake, D. R., Meinardi, S., and Pétron, G.: The Chemistry Mechanism in the Community Earth System Model Version 2 (CESM2), Journal of Advances in Modeling Earth Systems, 12, e2019MS001 882, https://doi.org/10.1029/2019MS001882, 2020.

Fast, J. D., Gustafson Jr., W. I., Easter, R. C., Zaveri, R. A., Barnard, J. C., Chapman, E. G., Grell, G. A., and Peckham, S. E.: Evolution of ozone, particulates, and aerosol direct radiative forcing in the vicinity of Houston using a fully coupled meteorology-chemistry-aerosol model, Journal of Geophysical Research: Atmospheres, 111, https://doi.org/10.1029/2005JD006721, 2006.

Gentry, B. M., Robinson, A. L., and Adams, P. J.: EASIUR-HR: A Model To Evaluate Exposure Inequality Caused by Ground-Level Sources of Primary Fine Particulate Matter, Environmental Science & Technology, 57, 3817–3824, https://doi.org/10.1021/acs.est.2c06317, pMID: 36802589, 2023.

Goodkind, A. L., Tessum, C. W., Coggins, J. S., Hill, J. D., and Marshall, J. D.: Fine-scale damage estimates of particulate matter air pollution reveal opportunities for location-specific mitigation of emissions, Proceedings of the National Academy of Sciences, 116, 8775–8780, https://doi.org/10.1073/pnas.1816102116, 2019.

Grell, G., Freitas, S. R., Stuefer, M., and Fast, J.: Inclusion of biomass burning in WRF-Chem: impact of wildfires on weather forecasts, Atmospheric Chemistry and Physics, 11, 5289–5303, https://doi.org/10.5194/acp-11-5289-2011, 2011.

Grell, G. A., Peckham, S. E., Schmitz, R., McKeen, S. A., Frost, G., Skamarock, W. C., and Eder, B.: Fully coupled “online” chemistry within the WRF model, Atmospheric Environment, 39, 6957–6975, https://doi.org/10.1016/j.atmosenv.2005.04.027, 2005.

Grell, G. A., Freitas, S. R., et al.: A scale and aerosol aware stochastic convective parameterization for weather and air quality modeling, Atmospheric Chemistry Physics, pp. 5233–5250, https://doi.org/10.5194/acp-14-5233-2014, 2014.

https://doi.org/10.5194/egusphere-2026-797
Preprint. Discussion started: 6 March 2026

Guenther, A., Jiang, X., Heald, C., Sakulyanontvittaya, T., Duhl, T., Emmons, L., and Wang, X.: The Model of Emissions of Gases and Aerosols from Nature version 2.1 (MEGAN2. 1): an extended and updated framework for modeling biogenic emissions, Geoscientific Model Development, 5, 1471–1492, https://doi.org/10.5194/gmd-5-1471-2012, 2012.

Heo, J., Adams, P. J., and Gao, H. O.: Public Health Costs of Primary PM2.5 and Inorganic PM2.5 Precursor Emissions in the United States, Environmental Science & Technology, 50, 6061–6070, https://doi.org/10.1021/acs.est.5b06125, pMID: 27153150, 2016.

Hong, S.-Y., Noh, Y., and Dudhia, J.: A new vertical diffusion package with an explicit treatment of entrainment processes, Monthly Weather Review, 134, 2318–2341, https://doi.org/10.1175/MWR3199.1, 2006.

Lin, Y.-L., Farley, R. D., and Orville, H. D.: Bulk parameterization of the snow field in a cloud model, Journal of Climate and Applied Meteorology, 22, 1065–1092, https://doi.org/10.1175/1520-0450(1983)022<1065:BPOTSF>2.0.CO;2, 1983.

McDuffie, E. E., Martin, R. V., Spadaro, J. V., Burnett, R., Smith, S. J., O'Rourke, P., Hammer, M. S., van Donkelaar, A., Bindle, L., Shah, V., Jaeglé, L., Luo, G., Yu, F., Adeniran, J. A., Lin, J., and Brauer, M.: Source sector and fuel contributions to ambient PM2.5 and attributable mortality across multiple spatial scales, Nature Communications, 12, https://doi.org/10.1038/s41467-021-23853-y, 2021.

Mendez-Espinosa, J. F., Belalcazar, L. C., and Morales-Betancourt, R.: Regional air quality impact of northern South America biomass burning emissions, Atmospheric Environment, 203, 131–140, https://doi.org/10.1016/j.atmosenv.2019.01.042, 2019.

Mlawer, E. J., Taubman, S. J., Brown, P. D., Iacono, M. J., and Clough, S. A.: Radiative transfer for inhomogeneous atmospheres: RRTM, a validated correlated-k model for the longwave, Journal of Geophysical Research: Atmospheres, 102, 16 663–16 682, https://doi.org/10.1029/97JD00237, 1997.

Morales Betancourt, R., Rojas Neisa, D. R., Piracoca, A., and Espitia Cano, S.: Supplementary Data for "Implementation of the reduced complexity model InMAP at urban scale using a high-resolution WRF-Chem simulation": WRF-Chem D03 2018 base simulation., DataHub, https://doi.org/10.71590/9RESNN, 2026.

NCEP: NCEP FNL Operational Model Global Tropospheric Analyses, continuing from July 1999, Research Data Archive at the National Center for Atmospheric Research, Computational and Information Systems Laboratory, 10.5065/D6M043C6, 2000.

Orellano, P., Reynoso, J., Quaranta, N., Bardach, A., and Ciapponi, A.: Short-term exposure to particulate matter (PM10 and PM2.5), nitrogen dioxide (NO2), and ozone (O3) and all-cause and cause-specific mortality: Systematic review and meta-analysis, Environment International, 142, 105 876, https://doi.org/https://doi.org/10.1016/j.envint.2020.105876, 2020.

Pachón, J. E., Galvis, B., Lombana, O., Carmona, L. G., Fajardo, S., Rincón, A., Meneses, S., Chaparro, R., Nedbor-Gross, R., and Henderson., B.: Development and evaluation of a comprehensive atmospheric emission inventory for air quality modeling in the megacity of Bogotá, Atmosphere, 9, https://doi.org/10.3390/atmos9020049, 2018.

Powers, J. G., Klemp, J. B., Skamarock, W. C., Davis, C. A., Dudhia, J., O, D. G., Coen, J. L., Gochis, D. J., Ahmadov, R., Peckham, S. E., et al.: The Weather Research and Forecasting Model: Overview, system efforts, and future directions, Bulletin of the American Meteorological Society, 98, 1717–1737, https://doi.org/10.1175/BAMS-D-15-00308.1, 2017.

Pérez-Peña, M. P., Henderson, B. H., Nedbor-Gross, R., and Pachón, J. E.: Natural mitigation factor adjustment for re-suspended particulate matter emissions inventory for Bogotá, Colombia, Atmospheric Pollution Research, 8, 29–37, https://doi.org/https://doi.org/10.1016/j.apr.2016.07.006, 2017.

Stockwell, W. R., Middleton, P., Chang, J. S., and Tang, X.: The second generation regional acid deposition model chemical mechanism for regional air quality modeling, Journal of Geophysical Research: Atmospheres, 95, 16 343–16 367, https://doi.org/https://doi.org/10.1029/JD095iD10p16343, 1990.

https://doi.org/10.5194/egusphere-2026-797
Preprint. Discussion started: 6 March 2026

Stockwell, W. R., Kirchner, F., Kuhn, M., and Seefeld, S.: A new mechanism for regional atmospheric chemistry modeling, Journal of Geophysical Research: Atmospheres, 102, 25 847–25 879, https://doi.org/https://doi.org/10.1029/97JD00849, 1997.

Tessum, C. W., Hill, J. D., and Marshall, J. D.: Twelve-month, 12 km resolution North American WRF-Chem v3.4 air quality simulation: performance evaluation, Geoscientific Model Development, 8, 957–973, https://doi.org/10.5194/gmd-8-957-2015, 2015.

Tessum, C. W., Hill, J. D., and Marshall, J. D.: InMAP: A model for air pollution interventions, PLOS ONE, 12, 1–26, https://doi.org/10.1371/journal.pone.0176131, 2017.

Tessum, M. W., Anenberg, S. C., Chafe, Z. A., Henze, D. K., Kleiman, G., Kheirbek, I., Marshall, J. D., and Tessum, C. W.: Sources of ambient PM2.5 exposure in 96 global cities, Atmospheric Environment, 286, 119 234, https://doi.org/https://doi.org/10.1016/j.atmosenv.2022.119234, 2022.

Thakrar, S. K., Tessum, C. W., Apte, J. S., Balasubramanian, S., Millet, D. B., Pandis, S. N., Marshall, J. D., and Hill, J. D.: Global, high-resolution, reduced-complexity air quality modeling for PM2.5 using InMAP (Intervention Model for Air Pollution), PLOS ONE, 17, 1–22, https://doi.org/10.1371/journal.pone.0268714, 2022.

Wheeler, S. M.: Built landscapes of metropolitan regions: An international typology, The Journal of the American Planning Association, 81, 167–190, https://doi.org/http://dx.doi.org/10.1080/01944363.2015.1081567, 2015.

WHO: WHO Air quality guidelines for particulate matter, ozone, nitrogen dioxide and sulfur dioxide : global update 2005 : summary of risk assessment, 2006.

Wiedinmyer, C., Akagi, S., Yokelson, R. J., Emmons, L., Al-Saadi, J., Orlando, J., and Soja, A.: The Fire INventory from NCAR (FINN): A high resolution global model to estimate the emissions from open burning, Geoscientific Model Development, 4, 625–641, https://doi.org/10.5194/gmd-4-625-2011, 2011.

Wu, R., Tessum, C. W., Zhang, Y., Hong, C., Zheng, Y., Qin, X., Liu, S., and Zhang, Q.: Reduced-complexity air quality intervention modeling over China: the development of InMAPv1.6.1-China and a comparison with CMAQv5.2, Geoscientific Model Development, 14, 7621–7638, https://doi.org/10.5194/gmd-14-7621-2021, 2021.